JOURNAL OF GEOPHYSICAL RESEARCH: BIOGEOSCIENCES, VOL. 118, 445–461, doi:10.1002/jgrg.20047, 2013

Contrasting CO_2 concentration discharge dynamics in headwater streams: A multi-catchment comparison

K. J. Dinsmore,[1] M. B. Wallin,[2] M. S. Johnson,[3,4] M. F. Billett,[1] K. Bishop,[2,5] J. Pumpanen,[6] and A. Ojala[7]

Received 20 March 2012; revised 22 February 2013; accepted 2 March 2013; published 3 April 2013.

[1] Aquatic CO_2 concentrations are highly variable and strongly linked to discharge, but until recently, measurements have been largely restricted to low-frequency manual sampling. Using new in situ CO_2 sensors, we present concurrent, high-frequency (<30 min resolution) CO_2 concentration and discharge data collected from five catchments across Canada, UK, and Fennoscandinavia to explore concentration-discharge dynamics; we also consider the relative importance of high flows to lateral aquatic CO_2 export. The catchments encompassed a wide range of mean CO_2 concentrations (0.73–3.05 mg C L^{-1}) and hydrological flow regimes from flashy peatland streams to muted outflows within a Finnish lake system. In three of the catchments, CO_2 concentrations displayed clear bimodal distributions indicating distinct CO_2 sources. Concentration-discharge relationships were not consistent across sites with three of the catchments displaying a negative relationship and two catchments displaying a positive relationship. When individual high flow events were considered, we found a strong correlation between both the average magnitude of the hydrological and CO_2 response peaks, and the average response lag times. An analysis of lateral CO_2 export showed that in three of the catchments, the top 30% of flow (i.e., flow that was exceeded only 30% of the time) had the greatest influence on total annual load. This indicates that an increase in precipitation extremes (greater high-flow contributions) may have a greater influence on the flushing of CO_2 from soils to surface waters than a long-term increase in mean annual precipitation, assuming source limitation does not occur.

Citation: Dinsmore, K. J., M. B. Wallin, M. S. Johnson, M. F. Billett, K. Bishop, J. Pumpanen, and A. Ojala (2013), Contrasting CO_2 concentration discharge dynamics in headwater streams: A multi-catchment comparison, *J. Geophys. Res. Biogeosci.*, *118*, 445–461, doi:10.1002/jgrg.20047.

1. Introduction

[2] Soils represent an important and dynamic store of global carbon which interacts with the atmospheric carbon pool either through direct soil-plant-atmosphere exchange or transport to and subsequent loss from the surface drainage system. Until recently, much of the literature has focused on the first of these pathways often ignoring losses through the drainage system [e.g., *Baldocchi et al.*, 2001; *Bubier et al.*, 2002; *Lafleur et al.*, 2003]. We currently have a relatively good understanding of the dynamics and hydrochemical processes that control concentrations and fluxes of dissolved organic carbon (DOC) in flowing surface waters [*Clark et al.*, 2007; *Hope et al.*, 1994; *McDowell and Likens*, 1988]. While the relative importance of gaseous evasion from surface waters to total catchment budgets is now recognised [*Butman and Raymond*, 2011; *Dinsmore et al.*, 2010; *Huotari et al.*, 2011; *Nilsson et al.*, 2008; *Richey et al.*, 2002], the processes which control temporal and spatial variability of CO_2 concentration (and hence the magnitude of the flux) are still not fully understood. Gaseous evasion therefore represents a significant source of uncertainty in greenhouse gas accounting. To fully understand catchment carbon budgets, all flux pathways need to be accounted for. Although lateral CO_2 export is often of a smaller magnitude than vertical evasion [*Dinsmore et al.*, 2010; *Wallin et al.*, 2013], it represents a loss of C from the terrestrial to the aquatic system and is therefore an important term to both quantify and understand.

[3] CO_2 supersaturation is common in most natural drainage networks across boreal, temperate, and tropical systems [*Aufdenkampe et al.*, 2011; *Cole et al.*, 1994; *Cole et al.*,

[1]Centre for Ecology and Hydrology, Bush Estate, Penicuik, UK.
[2]Department of Earth Sciences, Uppsala University, Uppsala, Sweden.
[3]Institute for Resources, Environment and Sustainability, University of British Columbia, Vancouver, British Columbia, Canada.
[4]Department of Earth, Ocean and Atmospheric Sciences, University of British Columbia, Vancouver, British Columbia, Canada.
[5]Department of Aquatic Sciences and Assessment, Swedish University of Agricultural Sciences, Uppsala, Sweden.
[6]Department of Forest Sciences, University of Helsinki, Helsinki, Finland.
[7]Department of Environmental Sciences, University of Helsinki, Lahti, Finland.

Corresponding author: K. J. Dinsmore, Centre for Ecology and Hydrology, Bush Estate, Penicuik EH26 0QB, UK. (kjdi@ceh.ac.uk)

2169-8953/13/10.1002/jgrg.20047

2007; *Kling et al*., 1991; *Richey et al*., 2002]. Estimates of CO_2 evasion rates from running waters (expressed per unit water surface area) cover a wide range of values, e.g., $1.65 \pm 0.21\,\mu g\,C\,m^{-2}\,s^{-1}$ from Arctic rivers [*Kling et al*., 1992] to $263 \pm 76.1\,\mu g\,C\,m^{-2}\,s^{-1}$ in Amazonian tropical forests [*Richey et al*., 2002], $21–806\,\mu g\,C\,m^{-2}\,s^{-1}$ in Scottish peatland catchments [*Dinsmore et al*., 2010; *Hope et al*., 2001; *Billett and Harvey*, 2012], and typically $10–300\,\mu g\,C\,m^{-2}\,s^{-1}$ in boreal streams [*Wallin et al*., 2011]. Contributions of stream/river CO_2 evasion to total catchment budgets have been estimated to equal up to 50% of net annual carbon accumulation in Arctic tundra [*Kling et al*., 1991], up to 70% in peatlands [*Hope et al*., 2001] and roughly equal to net annual carbon accumulation in the central floodplain region of the Amazon [*Richey et al*., 2002].

[4] The rate of gaseous evasion from surface waters is dependent on the solubility of the gas, the physical rate at which molecules can exchange across the water-air interface (given by the gas transfer coefficient or gas transfer velocity), and the water-air concentration gradient. Understanding the temporal dynamics and controls on CO_2 concentrations is therefore the essential first step in accurately quantifying and understanding evasion fluxes.

[5] Aquatic CO_2 can be derived from biogeochemical processes in the bedrock-soil system (weathering, decomposition of organic matter, root respiration) with dissolved CO_2 transported directly to the stream channel by runoff [*Billett et al*., 2007; *Johnson et al*., 2007]. In-stream bacterial and photo-chemical degradation of either terrestrial or aquatic derived substrate is an additional source of CO_2 [*Köhler et al*., 2002]. The relative importance of terrestrially derived carbon is both seasonal and site specific, with in-stream productivity restricted by cold temperatures, short in-stream residence times, low stream water pH, and stream bed characteristics [*Dubois et al*., 2010; *Raymond et al*., 1997; *Zeng and Masiello*, 2010]. Both the rate of carbon transport into the drainage system and the source-contribution area within the catchment are also highly temporally variable over shorter timescales in response to precipitation events [*Dinsmore and Billett*, 2008; *Rasilo et al*., 2012].

[6] The dominant hydrological flowpath through the catchment is dependent on the current and antecedent precipitation conditions. Hydrological flowpath dynamics control the areas within the catchment which are connected to the surface drainage network at any point in time. Due to the high degree of heterogeneity in biogeochemical processes within the terrestrial system and the resulting heterogeneity in carbon form and concentration, runoff chemistry is highly linked to source area and catchment flowpath dynamics [e.g., *Chapman et al*., 1999; *Nyberg*, 1995; *Wolock et al*., 1990]. The location of soil types within the catchment also significantly influences the degree to which they contribute to stream water concentrations. Stream water concentrations of biogenic CO_2 are generally higher where organic soils (rather than mineral soils) form alongside stream channels [*Wallin et al*., 2010]. The half life of in-stream CO_2 can be as little as a few hours [*Öquist et al*., 2009], and the contribution from upstream areas can drop quickly with distance from sampling location [*Rasilo et al*., 2012]. Catchment contributing area is therefore an important consideration when linking in-stream CO_2 concentrations to terrestrial sources and an important consideration when choosing a sampling location.

[7] Current climate predictions suggest a general increase in precipitation extremes across much of the globe, especially across tropical and northern regions where mean annual precipitation is also expected to increase [*Pachauri and Reisinger*, 2007]. Previous studies have shown that lateral aquatic carbon export is strongly biased towards high flow events [e.g., *Dinsmore and Billett*, 2008; *Dyson et al*., 2010; *Ojala et al*., 2011], so any increase in storm frequency or intensity is likely to impact the total CO_2 export from soils to surface waters. An understanding of stormflow CO_2 dynamics is therefore becoming increasingly important if we want to accurately quantify and predict catchment carbon losses via the aquatic pathway.

[8] Up to now, methodological limitations have restricted our knowledge of aquatic CO_2 dynamics, which is based on either low-frequency manual sampling techniques [e.g., *Billett and Moore*, 2008; *Billett et al*., 2004; *Dinsmore et al*., 2010; *Kling et al*., 1991] or inferred indirectly from the speciation of dissolved inorganic carbon concentrations [*Butman and Raymond*, 2011; *Maberly*, 1996; *Neal et al*., 1998; *Waldron et al*., 2007]. Data sets based on manual sampling techniques are inevitably of low temporal resolution and often biased toward low flow conditions, limiting their use for stormflow analysis. Even the indirect methods, which can be used to produce continuous CO_2 data sets, rely on alkalinity which itself is often measured on a spot sampling basis and therefore unlikely to provide sufficient information to accurately analyse high flows. The recent adaptation of high-frequency non-dispersive infrared sensors for use in aquatic systems has, for the first time, allowed direct and continuous measurements of CO_2 concentrations to be made in flowing water [*Johnson et al*., 2010].

[9] Previous studies have shown that the relationship between CO_2 and dissolved inorganic carbon (DIC) concentrations and discharge is generally negative [*Andrade et al*., 2011; *Billett et al*., 2004; *Dinsmore et al*., 2010; *Edwards*, 1973; *Edwards et al*., 1984; *Semiletov et al*., 2011; *Wallin et al*., 2010], although the strength and nature of the relationship are highly variable. For example, the role of pH in controlling the speciation of DIC (ratio between free CO_2, bicarbonates, carbonates, and carbonic acids) was suggested to counteract the reduction in CO_2 due to dilution in a number of streams monitored within the Krycklan catchment, Sweden [*Wallin et al*., 2010]. However, until the recent use of submerged sensor technology, relatively few direct measurements have been made across a sufficient hydrograph range to understand specific CO_2 stormflow dynamics. Where sensor technology has been utilized, the resulting chemographs show previously unseen intricacies, such as CO_2 pulses on the falling limb of the hydrographs [*Johnson et al*., 2007] or at peak flow [*Dinsmore and Billett*, 2008]; they also allow the quantification of response lags and determination of total stormflow exports.

[10] Here we combine aquatic time series data collected at five different northern hemisphere sites across northern Europe and Canada where CO_2 has been measured using submerged, in situ, CO_2 sensors during a series of storm events. The aim of this study, which uses consistent methodology and sensor type, is to compare and contrast the CO_2 concentration-discharge dynamics in individual streams and identify whether consistent relationships can be identified

across sites. Specifically, we aim to test the following hypotheses:

[11] (1) CO_2 concentrations are diluted during high flow events resulting in negative concentration-discharge relationships.

[12] (2) The form of the concentration-discharge relationship is linked to measurable catchment characteristics such as soil type or flow-duration indices.

[13] (3) The magnitude of the CO_2 response during individual storm events is correlated to the magnitude of the runoff response; the CO_2 response can therefore be predicted from hydrograph characteristics.

[14] (4) The lateral export of aquatic CO_2 from the upstream catchment area is strongly influenced by stormflow events as the effect of increased runoff counteracts the decrease in stream concentrations.

2. Methods

2.1. Site Descriptions

[15] We use data from five different study sites (Figure 1 and Table 1): the Malcom Knapp Research Forest (MK) in Maple Ridge, BC, Canada; the Black Burn draining Auchencorth Moss (AM) peatland, Scotland; Cottage Hill Sike (CHS) in the Moorhouse Reserve, England; Svartberget (SV) in the Vindeln Experimental Forests, Sweden; and the northern inlet of Lake Kuivajärvi near Hyytiälä (HY) SMEAR II (Station for Measuring Forest Ecosystem–Atmosphere Relations) field station, Finland. Site abbreviations (in brackets) will be used henceforth to reference individual field sites.

[16] The MK site is located within a 7 ha forested catchment in the coastal western hemlock climatic zone of BC, Canada. The site climatic conditions consist of mild, wet winters (mean January temperature 2.8°C) and warm dry summers (mean July temperature 17.2°C). The mean annual temperature and precipitation are9.6°C and 2200 mm y^{-1}, respectively [*Trubilowicz et al*., 2009].The catchment is dominated by western red cedar (*Thujaplicata*), Douglas-fir (*Pseudotsugamenziesii*), and western hemlock (*Tsugaheterophylla*). The catchment soil is a highly permeable humicpodzol consisting of an upper horizon of organic matter (< 10 cm), a sandy loam subsoil, and is underlain by glacial till over granitic bedrock [*Scordo and Moore*, 2009].

[17] Both AM (335 ha catchment) and CHS (17.4 ha catchment) are temperate oceanic peatland catchments within the UK. Mean annual air temperature and precipitation at AM are 8.1°C and 1155 mm, respectively (provided by M. Coyle, unpublished data, 2012). The mean annual temperature between 1931 and 2006 at Moor House weather station, 620 m from the CHS catchment, was 5.3°C. Mean annual precipitation was 2012 mm (records from 1951 to 1980 and 1991 to 2006) [*Holden and Rose*, 2011]. A typical winter in both AM and CHS will see several snowfall and melt events. AM vegetation is a mix of *Deschampsia flexuosa*, *Eriophorum vaginatum*, and *Juncus effusus* covering a base layer of *Sphagnum* mosses. The bedrock geology is Upper Carboniferous/Lower Devonian sandstones with occasional bands of limestone, mudstone, coal, and clay overlain by a thick layer of glacial boulder clay. CHS is lithologically similar to AM (Lower Carboniferous limestone, sandstone, and shale sequence overlain by glacial boulder clay) with vegetation consisting primarily of *Eriophorum vaginatum*, *Empetrum nigrum, Calluna vulgaris*, and *Sphagnum capillifolium*. Both catchments are dominated by histosols. A full carbon budget, including all aquatic carbon species, for AM has previously been published by *Dinsmore et al*. [2010]; aquatic carbon fluxes for CHS have been published in *Holden et al*. [2012].

[18] The SV site is located within a 50 ha forested catchment in boreal Sweden with an 8 ha headwater mire and another 2–3 ha of riparian peat in a 5–10 m wide strip adjacent to the stream. Mean annual air temperature (1980–2008) is 1.7°C with average temperatures in January and June of −9.6°C and 14.6°C, respectively. Mean annual precipitation (1981–2008) is 612 mm, with approximately 168 days of ground snow cover per year [*Haei et al*., 2010]. The forest vegetation is dominated by Norway spruce (*Piceaabies*) and Scots pine (*Pinussylvestris*) with an understory of *Calluna vulgaris, Vacciniumvitis*-idaea, and *Vacciniummyrtillus*. The 8 ha mire area is dominated by *Sphagnum* mosses. Soils are primarily podzolson glacial till formed from biotite plagioclase schist and orthogneiss

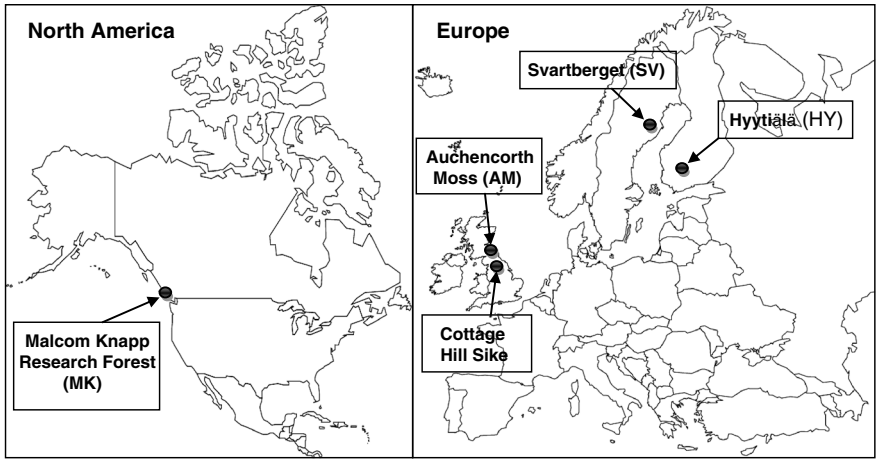

Figure 1. Location of study sites.

Table 1. Site Characteristics

	Vancouver Island (MK)	Auchencorth Moss (AM)	Cottage Hill Sike (CHS)	Svartberget (SV)	Hyytiälä (HY)
Location					
Country	Canada	UK	UK	Sweden	Finland
Lat/Long	49°26′ N; 122°55′W	55°47′N; 3°14′W	54°41′N; 2°23′W	64°14′N, 19°46′E	61°50′N; 24°17′E
Catchment Characteristics					
Cathment size (ha)	7	335	17	50	700–1000
Ecosystem type	Coastal Forest	Peatland	Peatland	Forest/Peat	Forest/Peat
Primary soil type	HumicPodzol	Histosol (85%)	Histosol	Podzol/Histosol	HaplicPodzol
Hydrology/Hydrochemistry					
Stream order	1	1	1	2	2
Mean annual runoff ratio	44%	77%	81%	50%	36–53%
Mean pH (range)	5.7 (5.4–6.0)	5.5 (4.3–7.3)	4.3 (3.8–7.2)	5.4 (4.2–6.0)	6.5 (6.0–6.7)
Mean conductivity (uS cm^{-1})	22.2	87.8	41.1	28.8	31.6
Climate Variables					
Climate zone	Coastal Western Hemlock	Subarctic oceanic	Subarctic oceanic	Boreal zone	Boreal zone
Mean annual temp. (°C)	9.6	8.1	5.3	1.7	2.9
Mean annual precip. (mm)	2200	1155	2012	612	692
Annual snow cover	NA[a]	NA	41 days yr^{-1}	168 days yr^{-1}	126

[a]Snow cover data not available for MK. Snowfall represents about 5% of annual precipitation at MK.

with histosols in the mire area and histic gleysolsin the 5–10 m wide riparian zone on either side of the stream. Lateral and evasive fluxes of CO_2, DIC, and DOC are presented in *Wallin et al*. [2013].

[19] The HY site drains a large catchment of approximately 700–1000 ha (estimated from contour map) consisting of both forest and mire. Mean annual air temperature and precipitation are 2.9°C, and 692 mm [*Ilvesniemi et al*., 2010], respectively, with an average of 126 days per year of ground snow cover in 2009 and 2010 compared to an average of 147 days from 2006 to 2011. The monitoring site is located at the northern inlet of Lake Kuivajärvi (surface area approximately 1 km^2), downstream of Lake Saarijärvi (area approximately 30 ha). The length of the stream between the two lakes is approximately 250 m. The vegetation consists of a mixture of Scots pine (*Pinussylvestris*) and Norway spruce (*Piceaabies*) with an understory of *Vaccinium myrtillus*, *Vaccinium vitis*-idaea, and *Rhododendron tomentosum* in the riparian wetlands; mosses *Dicra numpolysetum*, *Hylocomium splendens*, and *Pleurozium schreberi* on the uplands; and *Sphagnum spp*. on the riparian wetlands. Haplicpodzols overlie glacial till on granitic bedrock in the upland forests with histosols occurring in the riparian wetlands.

2.2. Methods

[20] CO_2 concentrations at all sites were monitored using GMT220 series non-dispersive infrared (NDIR) CO_2 transmitters manufactured by Vaisala (Helsinki, Finland), at a temporal frequency of < 30 min following the method described in *Johnson et al*. [2010]. Sensor accuracy is 1.5% of the calibrated range (0–1% CO_2) + 2% of the reading; this correlates to a maximum error of 0.33 mg C L^{-1} based on the maximum sensor reading measured at the CHS catchment. Sensors were enclosed in water-tight, gas-permeable PTFE membranes, deployed under the water surface (typically within a perforated PVC sleeve for protection) and connected to a data logger. Sensors were calibrated against known gas standards before and after deployment and corrected as appropriate; no signal drift was evident. Volume fraction outputs from the NDIR sensors were corrected for variations in temperature and pressure (atmospheric and water depth) using the method described in *Johnson et al*. [2010] and expressed in units of mg CO_2–C L^{-1}, hereafter annotated as mg C L^{-1}.

[21] Discharge and water temperature were measured concurrently with CO_2 concentration at each site. At MK, stream discharge was measured using a recording capacitance probe (TruTrack model WT-HR; Christ Church, New Zealand) located adjacent to a 90° V-notch weir at the watershed outlet. The TruTrack WT-HR sensor was also used to record air and water temperature. Both AM and CHS utilised Level TROLL® water level and temperature sensors (In-Situ Inc.). Discharge was calculated from a curvilinear stage-discharge rating curve (AM $r^2 = 0.97$; CHS $r^2 = 0.99$) built from a series of dilution gauging measurements. During periods of over-banking at CHS (3% of study period), discharge was extrapolated from a correlation with discharge at the nearby Trout Beck gauging station ($r^2 = 0.77$) provided by the UK "Environmental Change Network". Water level and temperature from SV was measured in a dam house with a V-notch weir using Campbell Scientific data loggers equipped with pressure transducers. Discharge was calculated from a stage-discharge rating curve based on a series of manual dilution gauging and bucket measurements ($r^2 > 0.90$). At HY, discharge was calculated using a relationship ($r^2 = 0.84$) between water level monitored continuously at half hour intervals using pressure sensors (Levelogger Gold, Solinst Canada Ltd., Gergetown, ON) and manual flow rate measurements (portable water velocity meter, Global Water FP111, Xylem Inc., White Plains, NY). Concentration data sets were not collected simultaneously across sites and therefore vary in both season and length. Monitoring periods for individual sites were as follwos: MK, April 2007–October 2008 (463 days); AM, October 2007–February 2008 (133 days); CHS, May–September 2009 (107 days); SV, April–November 2007 (215 days) and April–October 2008 (182 days); and HY, March–October 2010 (211 days).

[22] Continuous pH measurements were made alongside CO_2 at both MK (YSI 6000 multiparameter sonde) and AM (Campbell Scientific CSIM11 pH probe). A data set of weekly pH measurements from 1993 to 2007 at the CHS catchment was provided by the UK environmental change network (ECN). pH at HY was measured weekly

in 2010 and pH at SV weekly throughout 2007–2008 [*Wallin et al.*, 2010].

2.3. Data Analysis

[23] All concentrations are expressed in units of mg C L^{-1} and discharge in L s^{-1}. Site-specific export values represent lateral downstream transport calculated as the mean of hourly exports from instantaneous concentration multiplied by instantaneous discharge. Export values are given in units of g C per m^2 of catchment area per year (g C $m^{-2}\,yr^{-1}$), allowing for comparison between catchments of different size. Vertical CO_2 evasion is not estimated in this study.

[24] Hydrograph characteristic descriptions were based on daily mean discharges over the measurement period; hence, they do not necessarily represent long-term flow statistics. Descriptors include Q_{50}, Q_{90}, Q_{95}, Q_{10}, and Q_5 defined as the daily mean flow exceeded or equalled 50% (i.e., the median), 90%, 95%, 10%, or 5% of the time, respectively. $Q_{90}:Q_{50}$ ratios were calculated as a measure of low flow characteristics and $Q_{10}:Q_{50}$ as an additional normalised indication of high flow characteristics.

[25] Concentration-discharge relationships were examined using box plots of CO_2 concentrations within specified discharge exceedence limits (flow sectors), and the ratio of "flow weighted mean concentration" (FWMC) to unweightedCO_2 concentration. FWMC was calculated using equation (1) where c_i is the instantaneous concentration, q_i is the instantaneous discharge, and t_i is the time step between subsequent concentration measurements.

$$\mathrm{FWMC} = \sum(c_i \times t_i \times q_i)/\sum(t_i \times q_i) \tag{1}$$

[26] In the box-plot diagrams, the box represents the interquartile range with a line showing median CO_2 concentration. Whiskers extend to the highest/lowest data values within the upper/lower limit defined as 1.5 times the interquartile range. Outliers are defined as any data point beyond the upper/lower whisker limit; only the maximum and minimum outlier values are plotted. Hysteresis was examined by calculating the mean CO_2 concentration within the same discharge exceedence intervals as the box plots, separated into rising and falling limb data points. The statistical significance of the hysteresis was tested using paired *T*-tests on these discharge exceedence class means.

[27] CO_2 concentrations were modelled at each site utilising discharge and stream water temperature (the only two parameters that were available at the same temporal resolution as CO_2 concentration at all sites). Data sets were Ln-transformed where required to achieve a normal distribution. Lag terms of 1–10 h were applied to both temperature and discharge data sets; the lagged values were correlated with CO_2 concentrations, and the best fit parameter was taken forward to multiple regression models. Temperature was included as a model parameter at three temporal scales: (a) instantaneous, (b) mean over preceding day, and (c) mean over preceding week. Interaction terms between discharge and temperature were applied to all three temperature parameters. Model statistics represent the Pearson product moment correlation coefficient (Minitab version 16) comparing modelled versus measured CO_2 concentrations in a subset of randomly selected data points within the full time series. The size of the subset was defined by the degree of autocorrelation so that when ordered by date, no autocorrelation was present. For all sites except HY, a subset of 500 data points was randomly selected; for HY where autocorrelation was particularly strong, a smaller subset of 100 data points was selected.

[28] The classification of individual storm "events" was based on 30 day moving average hourly Q_{60} and Q_{20} values calculated for each stream individually. An event was classified as such if peak discharge exceeded the 30 day average Q_{20}. The start and end of the event were classified as the points at which the discharge exceeded and dropped below the 30 day average Q_{60}. This classification was devised through a process of adjustment (changing the threshold values) until events identified on visual inspection of all five data sets were suitably captured. Rising and falling hydrograph limbs are classified as time steps within the event classifications which are before or after the event hydrograph peaks, respectively.

[29] The following parameters were calculated for all individual events within the five discharge data sets: event duration, rising and falling limb durations, peak discharge, and "time since last" defined as the time between the start of the current event and the end of previous event. The individual CO_2 time series within each hydrologically defined event was then examined to identify any significant peaks or troughs. The following parameters were calculated from the CO_2 time series: CO_2 response defined as either the highest or lowest CO_2 concentration depending on whether a peak or trough was identified, relative CO_2 response defined as the CO_2 response divided by the mean CO_2 concentration over the full measurement period, and the concentration-discharge response lag defined as the time between discharge peak and peak CO_2 response. Relationships between individual event parameters within each catchment were examined using Pearson's product moment correlation analysis (Minitab® 16) on data sets transformed to fit a normal distribution. The mean of each event parameter was also calculated for each catchment, and the catchment means compared again using correlation analysis.

[30] DIC speciation was calculated using equation (2) where αH_2CO_3 is the proportion of dissolved carbonic acid (including both hydrated and dissolved CO_2). K_1 and K_2 are temperature-dependent dissociation constants calculated from equations (3) and (4) where T is temperature measured in units of Kelvin; constants a, b, and c are taken from [*Harned and Davis*, 1943; *Harned and Scholes*, 1941]

$$\propto H_2CO_3 = \frac{[H^+]^2}{[H^+]^2 + [H^+]K_1 + K_1K_2} \tag{2}$$

$$K = 10^{-pK} \tag{3}$$

$$pK = \frac{a}{T} + bT + c \tag{4}$$

3. Results

[31] Sites differed considerably in their discharge ranges (Table 2 and Figure 2); the lowest mean discharge values were recorded at MK and CHS (< 1 L s^{-1}), the highest

Table 2. Summary of Monitored Stream Variables Over Measurement Period[a]

Site	Mean Discharge (L s^{-1})	Mean Temp (°C)	Mean CO_2 (mg C L^{-1})	IQR (mg C L^{-1})	FWMC (mg C L^{-1})	Ratio Mean : FWMC
MK	0.71 (0–51.5)	8.17 ± 2.71	1.47 ± 0.19[a]	0.65	1.06	0.72
AM	19.9 (14.5–632)	4.36 ± 2.75	2.13 ± 0.17[b]	1.48	1.45	0.68
CHS	0.92 (0.67–371)	11.3 ± 2.26	3.05 ± 0.95[b]	1.95	1.61	0.53
SV	1.45 (0.48–137)	5.89 ± 3.19	0.96 ± 0.94[ac]	0.26	1.10	1.14
HY	97.9 (53.0–492)	13.2 ± 7.33	0.73 ± 0.54[c]	0.35	0.91	1.24

[a]Discharge values represent median and range, and both temperature and CO_2 are displayed as mean ± standard deviation. Groupings a, b, and c indicate groups where CO_2 concentrations overlap ± 1 standard deviation.

(97.9 L s^{-1}) at HY. MK was the only site where discharge <0.01 L s^{-1} was recorded; this occurred during an extended precipitation-free summer when the stream dried out completely. The highest mean CO_2concentration was measured at CHS (3.05 ± 0.95 mg C L^{-1}); it was statistically similar to both AM (2.13 ± 0.17 mg C L^{-1}) and the SV catchment in 2007 (0.93 ± 1.40 mg C L^{-1}) (Table 2). Although the mean CO_2 at SV during 2007 was lower than both MK and SV 2008, variability was high (Figure 3). The lowest mean CO_2 concentration was recorded in HY (0.73 ± 0.54 mg C L^{-1}).

[32] The calculation of DIC speciation based on temperature and pH showed that in all catchments, CO_2 was the major form of inorganic carbon (Figure 4). With the exception of HY, CO_2 represented a median proportion of >86% of all inorganic C species. The proportion of inorganic C represented by CO_2 in HY ranged from 31% to 78%. The greatest inter-quartile range was seen in AM, which despite a median of 94% CO_2 had a minimum of only16% CO_2. Based on the pH and temperature speciation, CO_3^{2-} was not present at any of the sample sites.

3.1. Hydrology

[33] Hydrographs over the full data collection periods are given in Figure 2 with hydrograph characteristics summarized in Table 3. HY had both the highest $Q_{90}:Q_{50}$ and lowest $Q_{10}:Q_{50}$ ratios indicating a relatively unresponsive catchment with a high base-flow contribution. The $Q_{10}:Q_{50}$ ratio suggested CHS is the most responsive/flashiest catchment.

[34] The number of high flow events recorded in the time series ranged from 8 in HY to 23 across the 2 year data set from SV. However, when corrected for the different time periods, the greatest frequency of events was observed in CHS, followed by AM, SV, MK, and HY, respectively (Table 4). The average event (using the classification given above) lasted from 3.1 days in CHS to 12.8 days in HY. The average event duration was directly correlated with the event frequency, following a negative power function ($r^2 = 0.98$, $p < 0.01$). Similarly, both rising and falling limb durations were negatively correlated with event frequency following power functions (rising $r^2 = 0.93$, $p = 0.02$; falling $r^2 = 0.98$, $p < 0.01$). In all catchments, the falling hydrograph limb was consistently >2 times longer than the rising limb.

3.2. Variability in CO_2 Concentrations

[35] CO_2 concentrations were highly variable across all time series (Figure 3); many of the catchments displayed not only large-scale spikes and troughs throughout the time series but also higher-frequency variability. This high-frequency variability was greatest in CHS and HY data sets collected in the summer season and lowest in AM (October to February). Frequency plots of CO_2 concentrations show clear bimodal distributions in MK (frequency peaks: 1.13 mg C L^{-1} and 2.42 mg C L^{-1}), SV (frequency peaks: 0.80 mg C L^{-1} and 1.02 mg C L^{-1}), and HY (frequency peaks: 0.59 mg C L^{-1} and 1.72 mg C L^{-1}) compared to the positively skewed distributions seen in both AM and CHS (Figure 5). AM and CHS also showed clear clustering of storm concentrations at the lower CO_2 range.

3.2.1. Concentration-Discharge Relationships

[36] To summarise concentration discharge relationships, the concentration data set was split into flow sectors based on discharge exceedence levels (Figure 6). The 0–10 discharge classes in Figure 6 represent the highest 0–10 % of flow, and the 90–100 class the lowest 0–10% of flow. Hence, the median CO_2 concentration decreases with increasing discharge classes in MK, AM, and CHS indicating a negative concentration-discharge relationship. The relationship is less clear in MK and CHS due to the large number of outliers. In SV, although there are outliers, a clear increase in median CO_2 concentration is evident in response to increasing discharge class indicating an overall positive concentration-discharge relationship. A general increase in CO_2 concentrations with increasing discharge class was observed in HY. However, removal of the 0–10 class, which relates almost entirely to snowmelt, significantly weakened this trend. The high CO_2 anomalies in the HY plot all represent points between 30 March 2010 and 01 May 2010, i.e., during the snowmelt period. CO_2 concentrations were high on the rising limb of the snowmelt event (Figure 3); hence, high concentrations from this period were evident across the full range of percentile groups.

[37] Similar discharge-dependent relationships were seen when the FWMC was compared to the unweighted mean concentrations (Table 2). A FWMC > unweighted mean indicates a positive concentration-discharge relationship; ratios of >1 were seen in SV (1.14) and HY (1.24), compared to ratios of <1 in MK (0.72), AM (0.68), and CHS (0.53).

[38] When data sets were split into rising or falling hydrograph limbs and the mean concentration within each percentile range plotted, hysteresis was evident (inferred from paired *T*-tests comparing rising and falling limbs) in four of the five catchments (Figure 6). Concentrations were significantly greater on the rising compared to the falling hydrograph limbs at the four sites. CHS was the only catchment in which hysteresis was not observed.

[39] CO_2 concentration models were fitted based on the observed discharge relationships and stream water temperature (Figure 3 and Table 5). Discharge was a significant

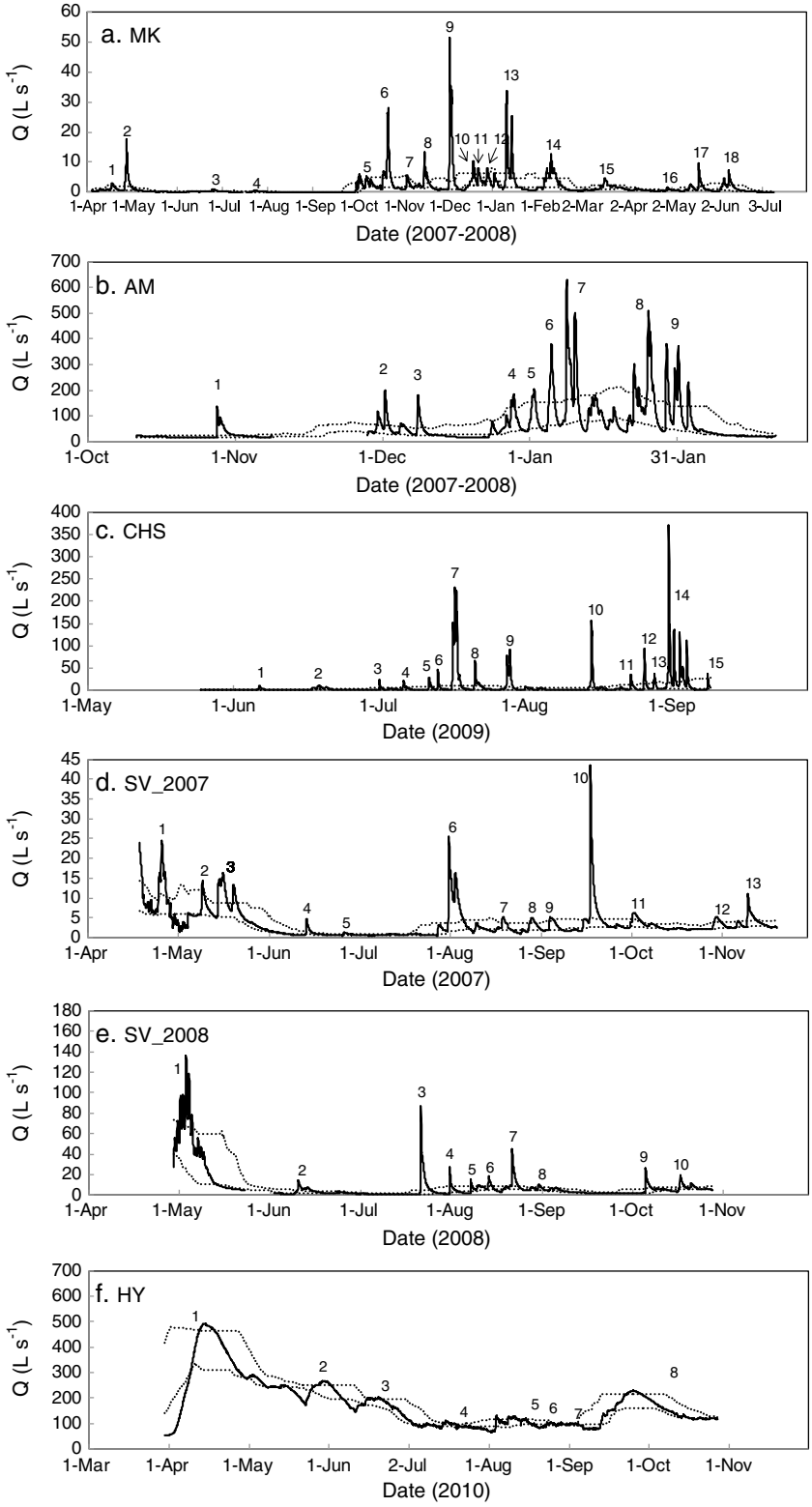

Figure 2. Hydrographs for individual sites during CO_2 monitoring period. Dashed lines refer to upper and lower storm classification thresholds. Numbers refer to individual storms.

parameter in models across all sites. In both AM and CHS discharge alone explained >70% of variability in the CO_2 concentration based on a power function; all other catchments were best modelled using multiple linear regression models. CO_2 concentrations at MK were relatively slow to respond to environmental parameters and were best modelled using a negative discharge function with a 9 h time lag and positive temperature averaged over the preceding week. Both SV and

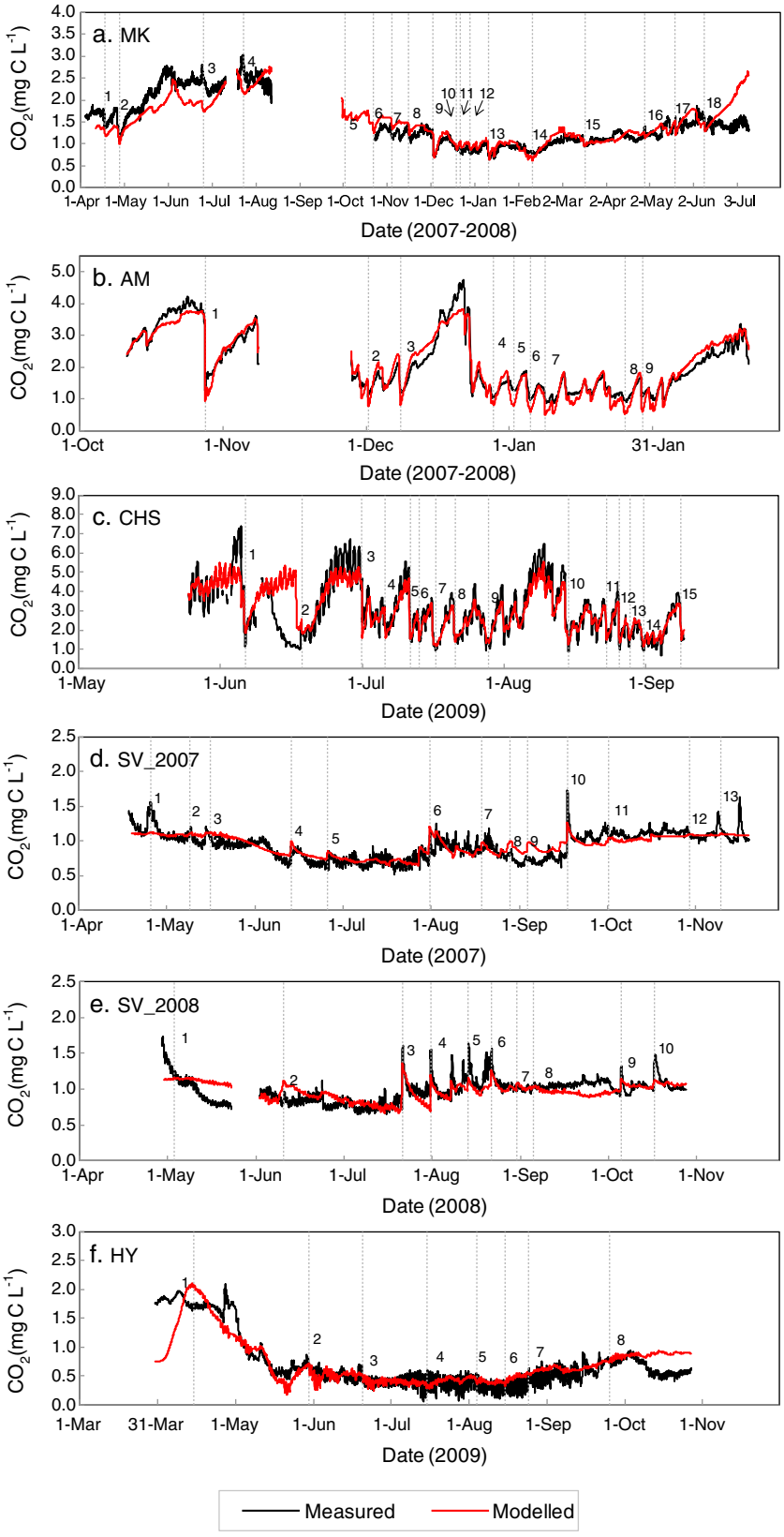

Figure 3. CO_2 time series for individual sites. Dashed lines and numbers refer to storm peaks identified in Figure 2.

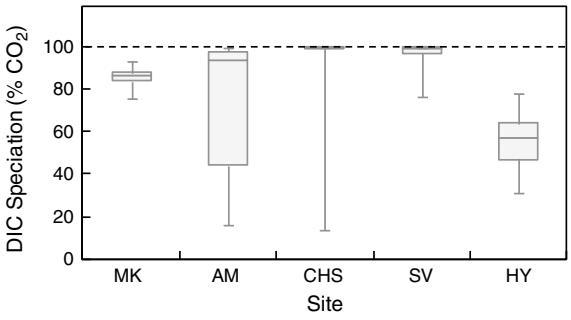

Figure 4. Box plots showing range DIC speciation ranges across individual sites. The box represents median and interquartile range; the whiskers represent range.

Table 3. Median Discharge for All Catchments Alongside High and Low Flow Hydrograph Descriptors Described in Text

	MK	AM	CHS	SV	HY
Median ($L\,s^{-1}$)	0.73	36.0	2.49	2.79	159
Low Flow Indices					
Q_{90}	0.00	16.7	0.81	0.74	86.6
Q_{95}	0.00	15.3	0.79	0.66	79.4
$Q_{90}:Q_{50}$	N/A	0.46	0.32	0.27	0.55
High Flow Indices					
Q_{10}	4.13	156	21.5	10.4	279
Q_5	6.24	203	45.4	17.4	380
$Q_{10}:Q_{50}$	5.68	4.33	8.61	3.72	1.76

HY displayed positive discharge relationships alongside a significant discharge-temperature interaction. However, while in SV the coincidence of high temperatures and high discharges resulted in high CO_2 concentrations, the opposite was true for HY.

3.2.2. Event Analysis

[40] Table 4 summarizes the CO_2 responses to individual storm events. The main CO_2 responses in MK, AM, and CHS were identified as troughs in the CO_2 time series; the main responses in SV and HY were identified as peaks. In both MK and AM, the response sometimes consisted of a trough with a small additional peak (events 3, 7, 9, 16, 17, and 18 in MK and events 2, 3, 4, 8, and 9 in AM Figure 3). In MK, the peak occurred just prior to the CO_2 dilution response, whereas in AM, the peak occurred at the base of the trough; examples of both are given in Figure 7. In some catchments, the number of CO_2 responses (n) was less than the number of identified events. Troughs and peaks were identified by visual inspection of the time-series data. For some events, particularly in the HY time series, the response was either masked by consistent diurnal variability or did not exist and could therefore not be included in the analysis. In all catchments except the lake inlet site HY (which was based on a sample size of only 4 events), the magnitude of the CO_2 response (peak/trough) was significantly correlated with the magnitude of the discharge peak (MK, $r = 0.55$, $p = 0.03$; AM, $r = 0.60$, $p < 0.01$; CHS, $r = 0.28$, $p = 0.02$; SV, $r = 0.46$, $p < 0.01$; HY, $r = 0.38$, $p = 0.24$).

[41] The peak/trough concentration relative to the mean CO_2 concentration (Table 2) was calculated to enable comparison between catchments (Table 4). The greatest relative CO_2 responses were seen in CHS and AM, followed by MK, SV, and HY, respectively, collectively showing a negative linear relationship with mean event duration ($r = 0.95$, $p = 0.01$). Within individual catchments, no relationship was seen between individual event duration and the magnitude of the CO_2 response. Furthermore, no relationships were found in any of the catchments between "time since last event" and CO_2 response.

[42] The lag between hydrological response and CO_2 response was greatest in HY, which took an average of ~2 days to react. In contrast, the fastest peak CO_2 response occurred in both AM and CHS ~20 min before the hydrograph peak. The variability in lag response time was extremely large among events with all catchments displaying both positive and negative lags, i.e., maximum CO_2 responses before and after peak discharge. Although within individual catchments there was no relationship between event duration and concentration-discharge response lag, when the mean concentration-discharge response lag of the five catchments was plotted against mean event duration

Table 4. Event Characteristics. CO_2 Response is Defined as Either the Highest or Lowest CO_2 Concentration Depending on Whether a Peak or Trough Was Identified[a]

	MK	AM	CHS	SV	HY
Hydrological Characteristics					
Total number events	18	9	15	23	8
Events per month	1.19	2.07	4.27	1.77	1.16
Event duration (days)	10.7 ± 1.58	6.24 ± 1.21	3.10 ± 0.50	8.34 ± 4.56	12.8 ± 3.42
Rising limb duration (days)	2.71 ± 0.6	1.64 ± 0.54	0.84 ± 0.23	1.88 ± 1.48	4.01 ± 1.42
Falling limb duration (days)	7.96 ± 1.29	4.6 ± 1.35	2.26 ±0.37	6.54 ± 4.42	8.81 ± 2.15
Peak height ($L\,s^{-1}$)	12.0 ± 3.48	6.76 ± 0.58	36.4 ± 9.15	10.9 ± 21.8	1.33 ± 0.06
CO_2 Response Characteristics					
Number of responses identified	16	9	15	23	4
Mean Event CO_2 ($mg\,L^{-1}$)	1.29 ± 0.15	2.04 ± 0.18	3.04 ± 0.03	0.94 ± 0.06	0.94 ± 0.08
1° CO_2 peak/trough concentration ($mg\,C\,L^{-1}$)	1.16 ± 0.13	1.07 ± 0.05	1.37 ± 0.11	1.24 ± 0.06	0.77 ± 0.07
2° CO_2 peak/trough concentration ($mg\,C\,L^{-1}$)	1.74 ± 0.226	1.16 ± 0.06	-	-	-
Relative peak/trough height ($mg\,C\,L^{-1}$)	0.31	1.06	1.68	0.28	0.04
Concentration-discharge response lag (hour)	17.9 ± 9.31	−0.33 ± 0.8	−0.33 ± 0.33	2.34 ± 7.02	47.8 ± 55.5

[a]Relative CO_2 response is defined as the CO_2 response divided by the mean CO_2 concentration over the full measurement period. The concentration-discharge response lag is defined as the time between discharge peak and peak CO_2 response.

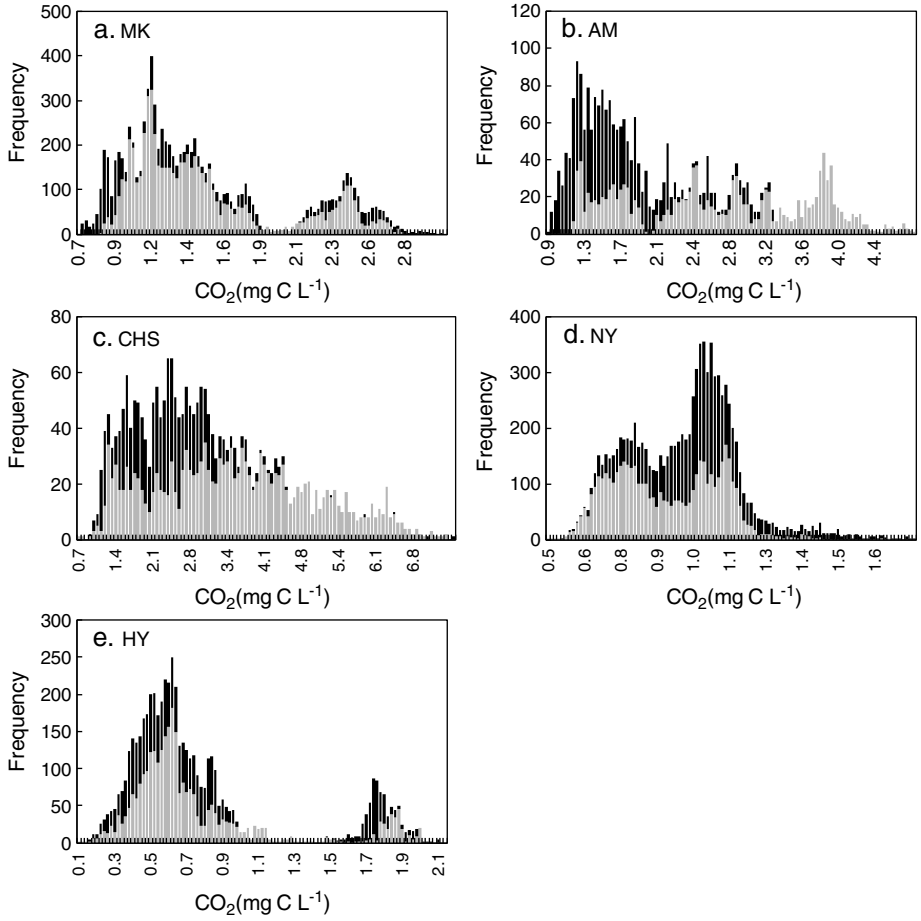

Figure 5. Frequency distributions of CO_2 concentrations identified as either storm (black bars) or non-storm (grey bars) data points.

for each catchment, there was a strong ($r = 0.91$, $p = 0.03$) positive logarithmic relationship. The relationship between concentration-discharge response lag was also strong with rising limb duration ($r = 0.96$, $p < 0.01$).

3.3. High Flow Contribution to Total CO_2 Export

[43] Plotting the percent of total CO_2 export against the discharge exceedence probability (the probability that discharge at a randomly selected time point will exceed a specified magnitude) provides a way of assessing the relative importance of different flow sectors (Figure 8a). The point where the plot shows the greatest deviation from the 1 : 1 line indicates the proportion of flow which is most significant to total CO_2 export. In HY, the greatest deviation occurred at approximately 70% equalled or exceeded discharge, and in SV approximately 50%, indicating low flow was proportionally more important to total CO_2 export than high flow. However, in the three first-order streams (AM, CHS, and MK), the greatest deviation and therefore the proportionally most important discharge sector was the top 30% of flow.

[44] CO_2 export is controlled by both CO_2 availability (both external source concentration and in situ production) and runoff, i.e., the volume of water available to transport the gas from one location to another. By plotting the percentage of total CO_2 export against the percentage of total runoff, we can distinguish between the influence of increased water flow and other contributing factors (Figure 8b). The 1 : 1 line indicates that CO_2 export within all flow sectors is controlled solely by discharge. Both HY and SV lie almost completely on top of one another and very slightly above the 1 : 1 line indicating that runoff was the primary factor controlling export. MK also follows the 1 : 1 line closely though sits beneath it. Both AM and CHS display concave curves, close to one another but below the 1 : 1 line.

4. Discussion

[45] We carried out this study in three first-order (MK, AM, and CHS) and two second-order (SV and HY) streams covering a range of flow regimes. The most distinct flow regime was seen in HY, characterized by the greatest base flow component ($Q_{90} : Q_{50} = 0.55$) and the smallest Q_{10} in relation to median flow ($Q_{10} : Q_{50} = 1.76$). This muted hydrological response is common in streams draining lake systems [e.g., *Spence*, 2006]. HY was also distinct in its DIC speciation pattern with the lowest proportion of inorganic carbon in the form of free CO_2. Both AM and CHS (UK peatland catchments) also had relatively high base flow components but were much more responsive to precipitation

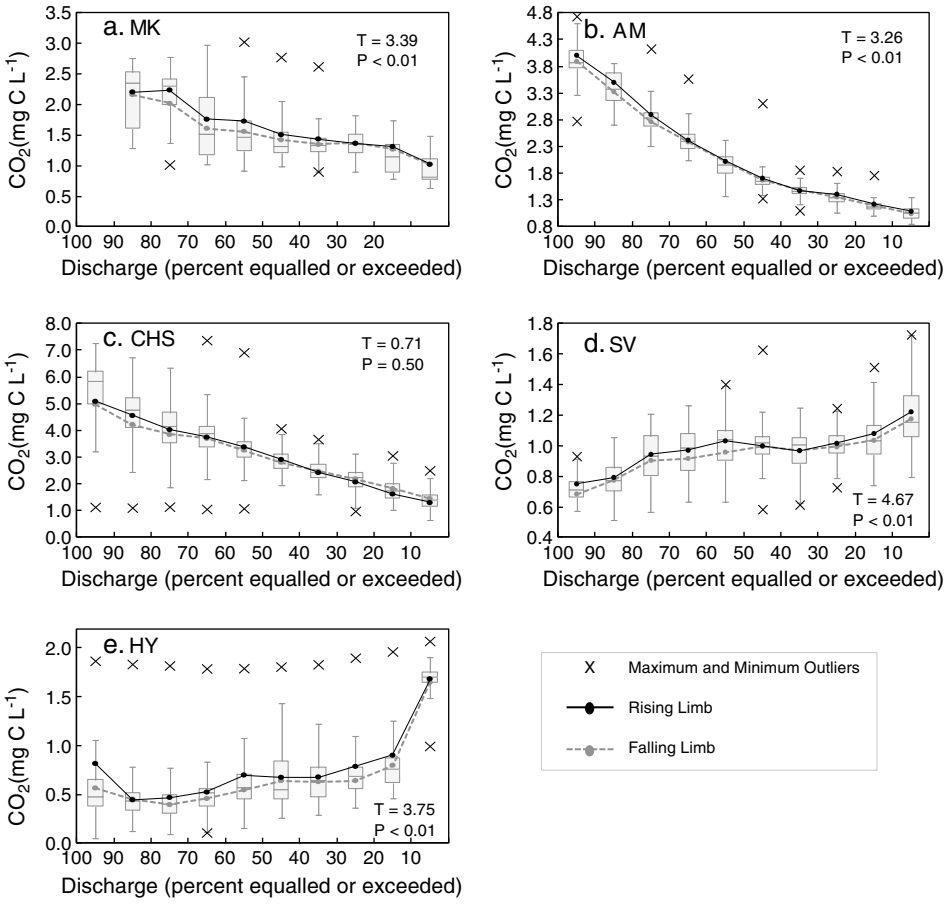

Figure 6. Box plots of concentrations split into discharge percentile classes with mean rising and falling limb concentrations shown to illustrate hysteresis. *T* and *p*-values represent statistical test for hysteresis.

Table 5. Best Fit Model Results for CO_2 Concentration Based on Discharge and Water Temperature

	Best Fit Model	Parameters/Equation	Coefficient
MK	Linear	Intercept	0.44
	(r = 0.86; p <0.01)	Ln(Discharge lag 9 hours)	−0.13
		Mean weekly temperature	0.12
AM	Power[a]	Ln(Discharge)	
	(r = 0.96; p <0.01)	α	37.6
		β	−2.32
CHS	Power[a]	(LnDischarge + 1)	
	(r = 0.71; p <0.01)	α	4
		β	−0.64
SV	Linear	Intercept	1.07
	(r = 0.67; p <0.01)	Ln(Discharge)	0.02
		Temperature	−0.03
		Interaction [Ln(Discharge) [a] Temperature]	0.01
HY	Linear	Intercept	0.58
	(r = 0.84; p <0.01)	Discharge	0.0035
		Interaction [Discharge [a] Temperature]	−0.00023

[a]Power function written in format $y = \alpha \cdot x \wedge \beta$ where α and β are model specific constants.

events reflecting the high water holding capacity of peat and the dominance of quick runoff pathways during rainfall events. MK was the only catchment to record zero flows (due to a highly seasonal precipitation regime) but again was highly responsive with an important high flow runoff contribution. SV had low base flow inputs and a $Q_{10}:Q_{50}$ ratio of only 3.72 (Table 3). Stream flashiness is influenced by a number of catchment parameters including catchment size, slope, and soil type but most notably in the comparison between the flashier UK streams (AM and CHS) and SV, it is influenced by the presence of tree cover in the latter which affects both evapotranspiration and interception, slowing the runoff response [e.g., *Bosch and Hewlett*, 1982].

[46] Mean CO_2 concentrations ranged from 0.73 mg C L^{-1} in HY to 3.05 mg C L^{-1} in CHS (Table 2); flow-weighted means ranged from 0.91 mg C L^{-1} in HY to 1.61 mg C L^{-1} in CHS. The only distinct grouping based on CO_2 concentrations was the two UK peatland sites, AM and CHS, where the highest CO_2 concentrations were measured. SV, which displayed the next highest FWMC, comprised approximately 16% mire [*Köhler et al*., 2008]. This supports work from *Wallin et al*. [2010] who found that peatland coverage was the most important predictor of aquatic CO_2 concentrations across 14 streams within the 67 km^2 Krycklan catchment. Although the HY catchment also contained peatland areas, it displayed the lowest FWMC (lower than the peat free MK catchment) possibly as a result of in-lake CO_2 consumption, which has previously been reported by *Kling et al*. [2000].This suggests that the presence of an upstream lentic environment was more important in controlling aquatic CO_2 concentrations than catchment characteristics at this site. However, the rate at which the lake CO_2 signal dissipates downstream, and therefore the strength of the signal at a particular sampling point, is likely to change seasonally in response to catchment inputs, aquatic carbon cycling, and discharge levels. Clearly, further work is required to generalise the influence of lentic systems on downstream CO_2 concentration dynamics.

[47] The greatest inter-quartile range, and therefore the "flashiest" CO_2 response, was seen in CHS, followed by AM, MK, HY, and SV, respectively (Table 2). Although not a statistically clear relationship, there appeared to be a link between hydrology and CO_2 variability, with CHS having the flashiest response for both. Furthermore, SV and HY, the two second-order streams with the most muted response to precipitation events, also displayed the least variability in CO_2concentration.

[48] The CO_2 concentrations in HY, MK, and SV all showed distinctive bimodal frequency distributions (Figure 5) suggesting distinct CO_2 sources. The higher CO_2 frequency peak in HY, centred around 1.72 mg C L^{-1}, could be isolated almost exclusively to the period prior to 1 May 2010 suggesting a linkage to snow melt runoff. This may reflect either CO_2 built up over the winter period under ice and snow or the direct input of snow melt-water which has previously been shown to contain high concentrations of CO_2 [*Dinsmore et al*., 2011a]. Again, the higher CO_2 frequency peak in MK can be linked to a specific time period—in this case, high concentrations relate to a period of low flow during summer 2007 (Figures 2 and 3)—suggesting a significant CO_2-rich base flow component with a median CO_2 concentration of

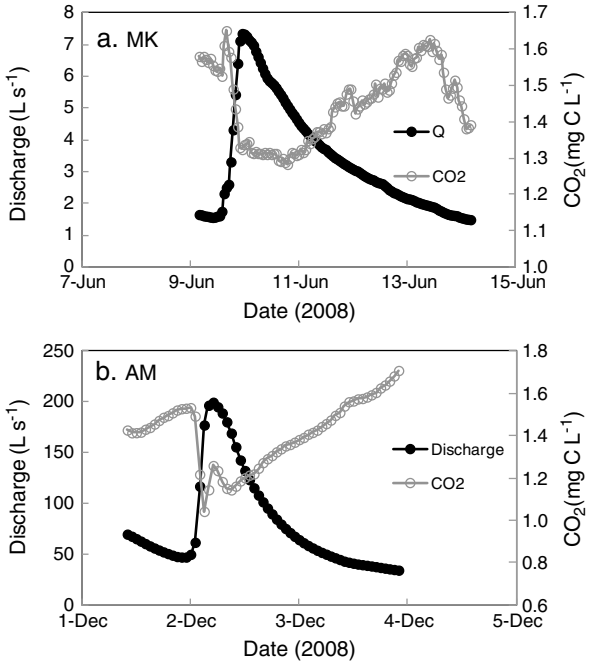

Figure 7. Example of secondary CO_2 peaks from (a) MK and (b) AM.

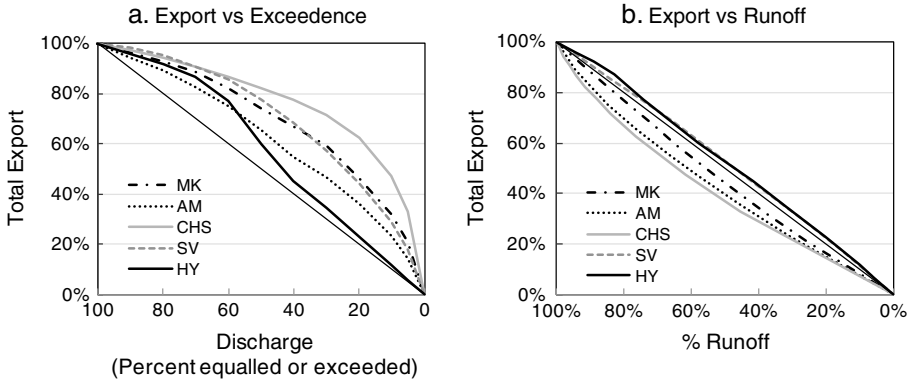

Figure 8. Plots of percent of total export against (a) percent of discharge displayed as exceedence probabilities and (b) percent of total runoff.

~2.42 mg C L^{-1}. No clear time period can be linked to the high concentration frequency peak in SV although there appears to be a dominance of event flow associated with the peak (Figure 5). We suggest this represents a source area within the catchment that has greater hydrological connectivity at periods of high flow. *Köhler et al.* [2008] describes a tributary 20 m upstream of the monitored SV site which became ephemeral during summer low flow and had a median CO_2 concentration more than double that measured at the monitoring site described in this study [*Wallin et al.*, 2010]. The high concentration CO_2 source (Figure 5) may therefore be the forested catchment drained by this tributary. Both AM and CHS have only one frequency peak despite the positively skewed distributions suggesting a more homogenous contributing source area.

4.1. Concentration-Discharge Relationships

[49] Although DOC concentrations display significant positive concentration-discharge relationships in many northern Hemisphere catchments associated with organo-mineral soils [*Hope et al.*, 1994]; the relationship does not hold true for many peatland streams [e.g., *Clark et al.*, 2008]. In contrast, DIC tends to show negative relationships with discharge [*Hope et al.*, 1994] linked to changing groundwater (weathering) contributions. Here we found that CO_2 concentrations in three of the five catchments also exhibited a negative concentration-discharge relationship.

[50] The negative concentration-discharge relationships in MK, AM, and CHS (Figure 6) all suggest a dilution of aquatic CO_2 concentrations at high flow in accordance with previous literature based on both CO_2 and DIC concentrations [*Andrade et al.*, 2011; *Billett et al.*, 2004; *Dinsmore et al.*, 2010; *Edwards*, 1973; *Edwards et al.*, 1984; *Semiletov et al.*, 2011; *Wallin et al.*, 2010]. The strength of the relationship (as indicated by the ratio of FWMC to unweighted mean concentration) appears to correlate negatively with mean stream water pH (Table 1), although with only three catchments this relationship cannot be tested statistically. A similar result was seen by *Wallin et al.* [2010] within the Krycklan catchment (Sweden) with the strongest negative relationships observed in the streams with the lowest pH. Streamwater CO_2 concentrations usually represent an integrated signal of multiple hydrological sources. The streamwater concentration is dependent on both the CO_2 concentrations in the source areas and, due to its influence on the carbonate equilibrium, the pH of the source water. Previous studies at AM have shown a strong negative pH-discharge relationship [*Dinsmore and Billett*, 2008], indicating a greater proportion of DIC is present as HCO_3^- during low flow. Despite this, the CO_2 concentration in the streamwater increases at low flow indicating that the CO_2 content of the low flow water source is high enough to mask the influence of speciation. No significant correlation was observed between CO_2 concentration and pH in the MK time series (based on a non-autocorrelated random subsample of 500 data points).

[51] CO_2 concentrations at both AM and CHS were best explained using discharge only (i.e., no temperature parameter) and reacted quickly to changes in discharge levels. In contrast, MK was slower to respond to discharge changes with the best concentration-discharge relationship achieved using a 9 h lag suggesting an initial input of highCO_2 concentration water, prior to dilution by recent event water. The concentration model for MK also included a positive term describing the average temperature over the preceding week. This suggests a link to recent biological activity rather than an influence of temperature dependent solubility, which would result in a negative relationship to instantaneous temperature such as that seen in SV.

[52] Distinct water sources can be either vertically distributed throughout the soil/bedrock profile or represent varying tributary discharge contributions in second-order streams such as SV. As previously discussed, the hydrological contribution from the CO_2-rich tributary upstream of the SV monitoring site is minor during summer low flows [*Köhler et al.*, 2008]. The greater proportion of total runoff originating from the CO_2-rich tributary during high flow may explain the positive concentration-discharge relationship (Figures 4 and 6).This highlights the importance of varying specific discharges from upstream tributaries in understanding the hydrochemistry of higher-order streams. It also highlights the importance of understanding water sources during site selection if a specific landscape interaction is being studied.

[53] The weak discharge relationship in HY is most likely explained by increased water residence time in the upstream lake system, which has previously been shown to obscure temporal signals in outlet nutrient dynamics [e.g. *Brown et al.*, 2008]. This causes a disconnect between the outflow stream water concentration and the catchment flow path dynamics, muting the overall concentration response. Furthermore, the presence of photosynthesis within the upstream lakes can decrease CO_2 concentrations [*Kling et al.*, 2000] and cause diurnal oscillations [*Hari et al.*, 2008], which may be a more important source of CO_2 variability than discharge responses in these systems. The temperature-discharge interaction model term complicates the interpretation further by suggesting that the co-occurrence of high temperature and high discharge results in lower streamwater CO_2 concentrations. Clearly, more parameters are needed to fully understand the CO_2 concentrations in the lake-stream continuum.

[54] All catchments with the exception of CHS displayed significant hysteresis in concentration-discharge relationships with rising limb concentrations greater than falling limb concentrations; this relationship holds true regardless of the sign of the concentration-discharge relationship. The interaction between CO_2 and pH, and CO_2 loss through turbulence-dependent evasion, makes the interpretation of CO_2 patterns complicated. Furthermore, *Dinsmore and Billett* [2008] showed that even within AM the hysteresis patterns across individual events were variable. Despite the aforementioned complexity, the presence of a significant relationship averaged over the full measurement period suggests that flushing and source depletion [*Johnson et al.*, 2007] were important controls on CO_2 dynamics in four of our study catchments.

4.2. "Event" Responses

[55] When specific CO_2 responses to individual events were analysed within each catchment, the only clear relationship that emerged was a correlation between discharge peak height and magnitude of CO_2 response. There was significant variability in CO_2 response among events which could not be explained with the available data. The

classification of an event in this study was based on parameters that could be applied equally across all catchments. In some circumstances, a single event under our classification actually contained a double hydrograph peak (particularly in MK, AM, and CHS where annual precipitation was high).This may have led to a break in the linkage between hydrology and CO_2 response and explain the lack of any clear correlations between event parameters. We used "time since last event" as a surrogate measure of antecedent conditions but found no correlation with CO_2 response. It is likely that a more precise measure of antecedent precipitation or soil moisture parameters may show a better relationship with CO_2 response. Despite the lack of clear relationships between events within a single catchment, when average event responses were considered across catchments, significant correlations to hydrological parameters were evident. The relative magnitude of the main CO_2 response and the concentration-discharge response lag were greatest in catchments with the shortest overall event duration; i.e., catchments with a flashier hydrology also showed the flashiest CO_2 responses.

[56] The lag between hydrological response and the response in CO_2 concentrations varied greatly between individual events. In all catchments, both positive and negative lags were seen indicating a peak CO_2 response on both rising and falling hydrograph limbs. Between catchments, however, a strong relationship existed between the response lag and both the overall event duration and particularly the rising limb duration. In AM and CHS where quick discharge responses (i.e.m short rising limbs) were common, lowest CO_2 concentration tended to occur before peak discharge. The quick runoff response indicated an initial dominance of surface or near-surface flow pathways. Due to the low catchment residence time of this event water, interaction with soil CO_2 stores is likely to be limited and result in a dilute source to the stream. As the event water begins to infiltrate, the dominance moves towards a slightly deeper through-flow component. This slower moving water has a greater opportunity to incorporate soil-derived CO_2, transporting it to the stream channel and raising stream concentrations. The timing of the switch between surface runoff pathways and deeper through-flow of infiltrated water will be catchment specific and control the concentration-discharge response lag.

[57] MK had a much longer rising limb duration suggesting a slower runoff response; this was also indicated by the 9 h lag in the model discharge parameter (Table 5). The soil type, forest cover, and catchment shape (long and narrow with the stream channel only in the lower half of the catchment) [*Trubilowicz et al*., 2009] are all characteristics that are likely to lead to greater rates of event water infiltration. Previous studies have shown that infiltrating event water can cause the displacement of CO_2-rich pre-event water [*Carey and Quinton*, 2004; *Inamdar et al*., 2004; *Johnson et al*., 2007]. In this scenario, the first water to reach the stream channel would be soil water displaced by piston flow which may explain the presence of a CO_2 peak prior to the dilution response. Once this soil water had been flushed out, the infiltrated event water would contain lower CO_2 concentrations and result in the observed dilution pattern. We would therefore expect to see a correlation between the presence/magnitude of the pre-dilution peak and antecedent soil moisture conditions; data were not available to test this hypothesis.

[58] Some of the events within AM displayed secondary CO_2 response peaks occurring at the base of the dilution trough (Figure 7). The AM response was previously explained by *Dinsmore and Billett* [2008] as an indication of variable contributing source areas and linkage to deeper peat at the catchment perimeter. A similar effect may have been occurring in SV which also contains an area of mire, likely to be a high CO_2 source, located ~1.1 km upstream from the main stream sampling point. CO_2 is also lost along the stream length through vertical evasion, with an estimated "half life" of 5.5 hrs in a headwater stream [*Öquist et al*., 2009; *Wallin et al*., 2011]. Therefore, the influence of upstream catchment areas and the likelihood of such a secondary peak arising is largely dependent on water residence time.

4.3. Contribution of High Flow to Total Lateral CO_2 Export

[59] Due to CO_2 source heterogeneity within catchment soil profiles, and the changing dominance of runoff flow-pathways across the hydrograph range, the relative importance of high versus low flow to total lateral CO_2 export varied between catchments. As current climate models predict not only future changes in total precipitation but changes in precipitation patterns, i.e., a move towards fewer rainfall events of greater intensities and magnitudes across northern regions [*Pachauri and Reisinger*, 2007], the need to understand the impact of changing flow regimes is increasing. Here we show that the proportion of flow with the greatest influence on total lateral export was the top 30% in MK, AM, and CHS. These three catchments displayed negative concentration-discharge relationships but had the highest $Q_{10}:Q_{50}$ hydrological ratios. At these three sites, an increase in precipitation extremes is likely to lead to a greater lateral export of aquatic CO_2 (within the limits of source CO_2 availability) than would be expected from a simple increase in mean annual precipitation alone. As CO_2 in headwater streams is primarily allochthonous in origin, lateral transport can be considered as a surrogate for the transport of CO_2 from the terrestrial to the aquatic system. Hence, an increase in precipitation extremes is likely to lead to a greater loss of terrestrialCO_2 to the aquatic system than an increase in mean annual precipitation alone. The relative contribution of the different flow sectors in SV was evenly distributed (Figure 8a), whereas in HY, it was clearly the low flow period that was most important for lateralCO_2 export (70% equalled or exceeded).

[60] If we only considered concentration-discharge relationships, we would expect high flow to be proportionally more important where a positive concentration-discharge relationship existed. Figure 8b illustrates that because of the concentration-discharge relationship, lateralCO_2 export across all flow sectors in MK, AM, and CHS was less than would have been expected due to increased runoff alone; the opposite was true in SV and HY. However, we find that hydrograph characteristics (and the associated catchment characteristics that define the hydrograph) appear to be more important than the concentration-discharge relationship in defining the specific flow sector contribution to total lateral export. Although it is difficult to draw numeric conclusions that can

be usefully upscaled from only five catchments, we have identified trends that could be explored empirically in other systems and potentially modelled. This could lead to a much better understanding of the influence of precipitation patterns on lateral CO_2 export, and more importantly, losses of CO_2 from the soil to the stream system where vertical evasion is the predominant flux pathway.

[61] Current methodological limitations prevent the measurement of gas transfer coefficients at a temporal resolution suitable to carry out a similar flow sector analysis on CO_2 losses through vertical evasion. As many previous studies have shown that the vertical evasion flux is often greater than lateral CO_2 losses [e.g., *Dinsmore et al*., 2010; *Wallin et al*., 2013], increasing the resolution of gas transfer coefficient measurements should be a future research priority and would enhance flux estimates particularly at high flow extremes.

4.4. Conclusions

[62] The highest CO_2 concentrations were measured at the two UK peatland dominated sites, AM and CHS, with the next highest FWMC at SV which contained ~16% mire. This supports previous work which concluded that peatland coverage was the most important predictor of aquatic CO_2 concentrations [*Wallin et al*., 2010; *Aitkenhead et al*., 1999]. Distinct bimodal frequency distributions in CO_2 concentration were observed in HY, MK, and SV. These suggest distinct CO_2 sources associated with (1) the snow melt period, (2) well-defined parts of the soil profile such as deep horizons which produce a stronger CO_2 signal at low flow, and (3) spatially separated subcatchments with variable tributary discharge contributions.

[63] Previous studies of aquatic C dynamics have shown significant positive DOC concentration-discharge relationships in organo-mineral soils and negative DIC concentration-discharge relationships associated with changing groundwater (weathering) contributions [e.g., *Hope et al*., 1994]. Here we found inconsistent CO_2 concentration-discharge relationships across sites. Negative relationships (Hypothesis 1) were seen in MK, AM, and CHS suggesting dilution of aquatic CO_2 at high flow. In contrast, SV displayed a positive concentration-discharge relationship. No clear relationship was seen in HY which was located within a lake system and where diurnal oscillations appeared to dominate CO_2 variability. The strength of the concentration-discharge relationship appeared to correlate negatively to stream water pH in AM, CHS, and MK; however, SV and HY illustrate that a more complex range of parameters is required to accurately predict the form of the concentration-discharge relationship. Since the range of processes that effect aquatic CO_2 in streams is clearly large, the ability to measure concentrations in situ and at high-frequency is greatly improving our understanding of its source, transport, and delivery to the stream system.

[64] CO_2 variability was strongly linked to hydrological variability with the "flashiest" response in both CO_2 concentration and the hydrograph occurring in CHS, and the least "flashy" responses in CO_2 occurring in SV and HY, which also displayed the most muted stream flow response to precipitation events. Correlations between hydrological and CO_2 responses in both response magnitude and lag were identified. Since concentration-discharge response lags were shortest in catchments with quick run-off responses, we suggest that the timing of the switch between surface runoff pathways (where present) and deeper through-flow of infiltrated water contributes to the concentration-discharge response lag.

[65] We show that the proportion of flow with the greatest influence on total lateral CO_2export was the top 30% in MK, AM, and CHS, indicating that an increase in event flow as a result of an increase in precipitation "extremes" will result in greater transport of terrestrial CO_2 to surface waters than would occur as a result of a simple increase in mean annual precipitation. The disparity in lateral export response between increasing mean precipitation and increasing extremes has important implications for carbon flux predictions based on future climate scenarios. The increase in lateral CO_2 export was linked to event flow runoff proportions rather than concentration-discharge relationships. It may therefore be possible in the future to use hydrographs to predict the relative importance of precipitation "extremes" to CO_2 export from individual catchments.

[66] **Acknowledgments.** The Canadian National Science and Engineering Research Council (NSERC) provided funding for the Canadian portion of the study. The UK portion of the study was funded by the UK Natural Environment Research Council (NERC) through an algorithm PhD studentship grant and grant NE/E003168/1. Financial support for the Swedish portion of this study was provided by the Swedish Research Council through a grant to K.B. (2005-4157) and as part of the Krycklan Catchment Study (KCS) which is funded by the Swedish Research Council, Form as (For Water), Future Forest, SKB, and the Kempe foundation. The Finnish part of the study was funded by the Academy of Finland, projects TRANSCARBO (1116347), FASTCARBON (130984), and the Centre of Excellence programme (project 1118615).

References

Aitkenhead, J. A., D. Hope, and M. F. Billett (1999), The relationship between dissolved organic carbon in stream water and soil organic carbon pools at different spatial scales, *Hydrol. Process.*, *13*(8), 1289–1302.

Andrade, T. M. B., P. B. Camargo, D. M. L. Silva, M. C. Piccolo, S. A. Vieira, L. F. Alves, C. A. Joly, and L. A. Martinelli (2011), Dynamics of dissolved forms of carbon and inorganic nitrogen in small watersheds of the coastal atlantic forest in Southeast Brazil, *Water Air Soil Pollut.*, *214*(1–4), 393–408, doi:10.1007/s11270-010-0431-z.

Aufdenkampe, A. K., E. Mayorga, P. A. Raymond, J. M. Melack, S. C. Doney, S. R. Alin, R. E. Aalto, and K. Yoo (2011), Riverine coupling of biogeochemical cycles between land, oceans, and atmosphere, *Front. Ecol. Environ.*, *9*(1), 53–60, doi:10.1890/100014.

Baldocchi, D., et al. (2001), FLUXNET: A new tool to study the temporal and spatial variability of ecosystem-scale carbon dioxide, water vapor, and energy flux densities, *Bull. Am. Meteorol. Soc.*, *82*(11), 2415–2434, doi:10.1175/1520-0477(2001)082<2415:FANTTS>2.3.CO;2.

Billett, M. F., M. H. Garnett, and F. Harvey (2007), UK peatland streams release old carbon dioxide to the atmosphere and young dissolved organic carbon to rivers, *Geophys. Res. Lett.*, *34*, L23401, doi:10.1029/2007GL031797.

Billett, M. F., and T. R. Moore (2008), Supersaturation and evasion of CO_2 and CH_4 in surface waters at Mer Bleue peatland, Canada, *Hydrol. Process.*, *22*, 2044–2054, doi:10.1002/hyp.6805.

Billett, M. F., S. M. Palmer, D. Hope, C. Deacon, R. Storeton-West, K. J. Hargreaves, C. Flechard, and D. Fowler (2004), Linking land-atmosphere-stream carbon fluxes in a lowland peatland system, *Global Biogeochem. Cycles*, *18*, GB1024, doi:10.1029/2003GB002058.

Billett M. F., and F. H. Harvey (2012), Measurements of CO_2 and CH_4 evasion from UK peatland headwater streams, *Biogeochemistry*, doi:10.1007/s10533-012-9798-9. Published online 05 October 2012.

Bosch, J. M., and J. D. Hewlett (1982), A review of catchment experiments to determine the effect of vegetation changes on water yield and evapotranspiration, *J. Hydrol.*, *55*(1–4), 3–23, doi:10.1016/0022-1694(82)90117-2.

Brown, P. D., W. A. Wurtsbaugh, and K. R. Nydick (2008), Lakes and forests as determinants of downstream nutrient concentrations in small mountain watersheds, *Arct. Antarct. Alp. Res.*, *40*(3), 462–469.

Bubier, J., P. Crill, and A. Mosedale (2002), Net ecosystem CO_2 exchange measured by autochambers during the snow-covered season at a temperate peatland, *Hydrol. Process.*, *16*, 3667–3682, doi:10.1002/hyp.1233.

Butman, D., and P. A. Raymond (2011), Significant efflux of carbon dioxide from streams and rivers in the United States, *Nat. Geosci.*, *4*(12), 839–842, doi:10.1038/ngeo1294.

Carey, S. K., and W. L. Quinton (2004), Evaluating snowmelt runoff generation in a discontinuous permafrost catchment using stable isotope, hydrochemical and hydrometric data, *Nord. Hydrol.*, *35*(4), 309–324.

Chapman, P. J., B. Reynolds, and H. S. Wheater (1999), Sources and controls of calcium and magnesium in storm runoff: The role of groundwater and ion exchange reactions along water flowpaths, *Hydrol. Earth Syst. Sci.*, *1*(3), 671–685, doi:10.5194/hess-1-671-1997.

Clark, J. M., S. N. Lane, P. J. Chapman, and J. K. Adamson (2007), Export of dissolved organic carbon from an upland peatland during storm events: Implications for flux estimates, *J. Hydrol.*, *347*(3–4), 438–447, doi:10.1016/j.jhydrol.2007.09.030.

Clark, J. M., S. N. Lane, P. J. Chapman, and J. K. Adamson (2008), Link between DOC in near surface peat and stream water in an upland catchment, *Sci. Total. Environ.*, *404*(2-3), 308–315, doi:10.1016/j.scitotenv.2007.11.002.

Cole, J. J., N. F. Caraco, G. W. Kling, and T. K. Kratz (1994), Carbon-dioxide supersaturation in the surface waters of lakes, *Science*, *265*(5178), 1568–1570, doi:10.1126/science.265.5178.1568.

Cole, J. J., et al. (2007), Plumbing the global carbon cycle: Integrating inland waters into the terrestrial carbon budget, *Ecosystems*, *10*(1), 171–184, doi:10.1007/s10021-006-9013-8.

Dinsmore, K. J., and M. F. Billett (2008), Continuous measurement and modelling of CO_2 losses from a peatland stream during stormflow events, *Water Resour. Res.*, *44*, W12417, doi:10.1029/2007WR007284.

Dinsmore, K. J., M. F. Billett, U. Skiba, R. M. Rees, J. Drewer, and C. Helfter (2010), Role of the aquatic pathway in the carbon and greenhouse gas budgets of a peatland catchment, *Glob. Chang. Biol.*, *16*(10), 2750–2762, doi:10.1111/j.1365-2486.2009.02119.x.

Dinsmore, K. J., M. F. Billett, K. E. Dyson, F. Harvey, A. M. Thomson, S. Piirainen, and P. Kortelainen (2011a), Stream water hydrochemistry as an indicator of carbon flow paths in Finnish peatland catchments during a spring snowmelt event, *Sci. Total. Environ.*, *409*(22), 4858–4867, doi:10.1016/j.scitotenv.2011.07.063.

Dubois, K. D., D. Lee, and J. Veizer (2010), Isotopic constraints on alkalinity, dissolved organic carbon, and atmospheric carbon dioxide fluxes in the Mississippi River, *J. Geophys. Res.*, *115*(G2), G02018, doi:10.1029/2009jg001102.

Dyson, K. E., M. F. Billett, F. Harvey, K. J. Dinsmore, A. M. Thomson, S. Piirainen, and P. Kortelainen (2010), Release of carbon and GHGs from peatland catchments in E Finland during the spring snow melt event, *Biogeochemistry*, doi:10.1007/s10533-010-9452-3.

Edwards, A. C., J. Creasey, and M. S. Cresser (1984), The conditions and frequency of sampling for elucidation of transport mechanisms and element budgets in upland drainage basins, paper presented at Proceedings of the International Symposium on Hydrochemical Balances of Freshwater Systems, Uppsala, Sweden.

Edwards, A. M. C. (1973), The variation of dissolved constituents with discharge in some norfolk rivers, *J. Hydrol. (Amsterdam)*, *18*(3–4), 219–242, doi:10.1016/0022-1694(73)90049-8.

Haei, M., M. G. Oquist, I. Buffam, A. Agren, P. Blomkvist, K. Bishop, M. O. Lofvenius, and H. Laudon (2010), Cold winter soils enhance dissolved organic carbon concentrations in soil and stream water, *Geophys. Res. Lett.*, *37*(5), L08501, doi:10.1029/2010gl042821.

Hari, P., J. Pumpanen, J. Huotari, P. Kolari, J. Grace, T. Vesala, and A. Ojala (2008), High-frequency measurements of productivity of planktonic algae using rugged nondispersive infrared carbon dioxide probes, *Limnol. Oceanogr. Methods*, *6*, 347–354.

Harned, H. S., and R. Davis (1943), The ionization constant of carbonic acid in water and the solubility of carbon dioxide in water and aqueous salt solutions from 0°C to 50°C, *J. Am. Chem. Soc.*, *65*, 2030–2037.

Harned, H. S., and S. R. Scholes (1941), The ionization constant of HCO_3^- from 0°C to 50°C, *J. Am. Chem. Soc.*, *63*, 1706–1709.

Holden, J., R. P. Smart, K. J. Dinsmore, A. J. Baird, M. F. Billett, and P. J. Chapman (2012), Natural pipes in blanket peatlands: major point sources for the release of carbon to the aquatic system, *Glob. Chang. Biol.*, *18*(12), 3568–3580,doi:10.1111/gcb.12004.

Holden, J., and R. Rose (2011), Temperature and surface lapse rate change: A study of the UK's longest upland instrumental record, *Int. J. Climatol.*, *31*, 907–919, doi:10.1002/joc.2136

Hope, D., M. F. Billett, and M. S. Cresser (1994), A review of the export of carbon in river water: Fluxes and processes, *Environ. Pollut.*, *84*, 301–324, doi:10.1016/0269-7491(94)90142-2.

Hope, D., S. M. Palmer, M. F. Billett, and J. J. C. Dawson (2001), Carbon dioxide and methane evasion from a temperate peatland stream, *Limnol. Oceanogr.*, *46*(4), 847–857.

Huotari, J., A. Ojala, E. Peltomaa, A. Nordbo, S. Launiainen, J. Pumpanen, T. Rasilo, P. Hari, and T. Vesala (2011), Long-term direct CO_2 flux measurements over a boreal lake: Five years of eddy covariance data, *Geophys. Res. Lett.*, *38*(5), L18401, doi:10.1029/2011gl048753.

Ilvesniemi, H., et al. (2010), Water balance of a boreal Scots pine forest, *Boreal Environ. Res.*, *15*(4), 375–396.

Inamdar, S. P., S. F. Christopher, and M. J. Mitchell (2004), Export mechanisms for dissolved organic carbon and nitrate during summer storm events in a glaciated forested catchment in New York, USA, *Hydrol. Process.*, *18*(14), 2651–2661, doi:10.1002/hyp.5572.

Johnson, M. S., M. F. Billett, K. J. Dinsmore, M. Wallin, K. E. Dyson, and R. S. Jassal (2010), Direct and continuous measurement of dissolved carbon dioxide in freshwater aquatic systems—Methods and applications, *Ecohydrology*, *3*, 68–78, doi:10.1002/eco.95.

Johnson, M. S., M. Weiler, E. G. Couto, S. J. Riha, and J. Lehmann (2007), Storm pulses of dissolved CO_2 in a forested headwater Amazonian stream explored using hydrograph separation, *Water Resour. Res.*, *43*(11), W11201, doi:10.1029/2007wr006359.

Kling, G. W., G. W. Kipphut, and M. C. Miller (1991), Arctic lakes and streams and gas conduits to the atmosphere: Implications for tundra carbon budgets, *Science*, *251*, 298–301, doi:10.1126/science.251.4991.298.

Kling, G. W., G. W. Kipphut, and M. C. Miller (1992), The flux of CO_2 and CH_4 from lakes and rivers in arctic Alaska, *Hydrobiologia*, *240*(1–3), 23–36, doi:10.1007/BF00013449.

Kling, G. W., G. W. Kipphut, M. M. Miller, and W. J. O'Brien (2000), Integration of lakes and streams in a landscape perspective: The importance of material processing on spatial patterns and temporal coherence, *Freshw. Biol.*, *43*(3), 477–497, doi:10.1046/j.1365-2427.2000.00515.x.

Köhler, S., I. Buffam, A. Jonsson, and K. Bishop (2002), Photochemical and microbial processing of stream and soilwater dissolved organic matter in a boreal forested catchment in northern Sweden, *Aquat. Sci.*, *64*(3), 269–281, doi:10.1007/s00027-002-8071-z.

Köhler, S. J., I. Buffam, H. Laudon, and K. H. Bishop (2008), Climate's control of intra-annual and interannual variability of total organic carbon concentration and flux in two contrasting boreal landscape elements, *J. Geophys. Res.*, *113*(G3), G03012, doi:10.1029/2007jg000629.

Lafleur, P. M., N. T. Roulet, J. L. Bubier, S. Frolking, and T. R. Moore (2003), Interannual variability in the peatland-atmosphere carbon dioxide exchange at an ombrotrophic bog, *Global Biogeochem. Cycles*, *17*(2), 1036, doi:10.1029/2002GB001983.

Nyberg, L. (1995), Water flow path interactions with soil hydraulic properties in till soil at Gårdsjön, Sweden, *J. Hydrol.*, *170*(1–4), 255–275, doi:10.1016/0022-1694(94)02667-Z.

Maberly, S. C. (1996), Diel, episodic and seasonal changes in pH and concentrations of inorganic carbon in a productive lake, *Freshw. Biol.*, *35*(3), 579–598.

McDowell, W. H., and G. E. Likens (1988), Origin, composition and flux of dissolved organic carbon in the Hubbard Brook valley, *Ecol. Monogr.*, *58*, 177–195.

Neal, C., M. Harrow, and R. J. Williams (1998), Dissolved carbon dioxide and oxygen in the River Thames: Spring-Summer 1997, *Sci. Total. Environ.*, *210–211*, 205–217, doi:10.1016/S0048-9697(98)00013-8.

Nilsson, M., J. Sagerfors, I. Buffam, H. Laudon, T. Eriksson, A. Grelle, L. Klemedtsson, P. Weslien, and A. Lindroth (2008), Contemporary carbon accumulation in a boreal oligotrophic minerogenic mire—A significant sink after accounting for all C-fluxes, *Glob. Chang. Biol.*, *14*(10), 2317–2332, doi:10.1111/j.1365-2486.2008.01654.x.

Ojala, A., J. López Bellido, T. Tulonen, P. Kankaala, and J. Huotari (2011), Carbon gas fluxes from a brown-water and a clear-water lake in the boreal zone during a summer with extreme rain events, *Limnol. Oceanogr.*, *56*, 61–76, doi:10.4319/lo.2011.56.1.0061.

Öquist, M. G., M. Wallin, J. Seibert, K. Bishop, and H. Laudon (2009), Dissolved inorganic carbon export across the soil/stream interface and its fate in a boreal headwater stream, *Environ. Sci. Technol.*, *43*(19), 7364–7369, doi:10.1021/es900416h.

Pachauri, R. K., and A. Reisinger (2007), Observed effects of climate change, in *Intergovernmental Panel on Climate Change. Climate Change 2007: Synthesis Report*., edited, pp. 31–33, IPCC, Geneva, Switzerland.

Rasilo, T., A. Ojala, J. Huotari, and J. Pumpanen (2012), Rain induced changes in carbon dioxide concentrations in the soil-lake-brook continuum of a boreal forested catchment, *Vadose Zone J.*, doi:10.2136/vzj2011.0039.

Raymond, P. A., N. F. Caraco, and J. J. Cole (1997), Carbon dioxide concentration and atmospheric flux in the Hudson river, *Estuaries*, *20*(2), 381–390.

Richey, J. E., J. M. Melack, A. K. Aufdenkampe, V. M. Ballester, and L. L. Hess (2002), Outgassing from the Amazonian rivers and wetlands as a large tropical source of atmospheric CO2, *Nature*, *416*, 617–620.

Scordo, E. B., and R. D. Moore (2009), Transient storage processes in a steep headwater stream, *Hydrol. Process.*, *23*(18), 2671–2685, doi:10.1002/hyp.7345.

Semiletov, I. P., I. I. Pipko, N. E. Shakhova, O. V. Dudarev, S. P. Pugach, A. N. Charkin, C. P. McRoy, D. Kosmach, and O. Gustafsson (2011),

Carbon transport by the Lena River from its headwaters to the Arctic Ocean, with emphasis on fluvial input of terrestrial particulate organic carbon vs. carbon transport by coastal erosion, *Biogeosciences*, *8*(9), 2407–2426, doi:10.5194/bg-8-2407-2011.

Spence, C. (2006), Hydrological processes and streamflow in a lake dominated watercourse, *Hydrol. Process.*, *20*(17), 3665–3681, doi:10.1002/hyp.6381.

Trubilowicz, J., K. Cai, and M. Weiler (2009), Viability of motes for hydrological measurement, *Water Resour. Res.*, *45*(6), W00d22, doi:10.1029/2008wr007046.

Waldron, S., E. M. Scott, and C. Soulsby (2007), Stable isotope analysis reveals lower-order river dissolved inorganic carbon pools are highly dynamic, *Environ. Sci. Technol.*, *41*(17), 6156–6162, doi:10.1021/es0706089.

Wallin, M., I. Buffam, M. Oquist, H. Laudon, and K. Bishop (2010), Temporal and spatial variability of dissolved inorganic carbon in a boreal stream network: Concentrations and downstream fluxes, *J. Geophys. Res. Biogeosci.*, *115*, G02014, doi:10.1029/2009jg001100.

Wallin, M. B., T. Grabs, I. Buffam, H. Laudon, A. Ågren, M. G. Öquist, and K. Bishop (2013), Evasion of CO_2 from streams—The dominant component of the carbon export through the aquatic conduit in a boreal landscape, *Glob. Chang. Biol.*, *19*(3), 785–797, doi:10.1111/gcb.12083.

Wallin, M. B., M. G. Öquist, I. Buffam, M. F. Billett, J. Nisell, and K. H. Bishop (2011), Spatiotemporal variability of the gas transfer coefficient $K(CO_2)$ in boreal streams: Implications for large scale estimates of CO_2 evasion, *Global Biogeochem. Cycles*, *25*(14), Gb3025, doi:10.1029/2010gb003975.

Wolock, D. M., G. M. Hornberger, and T. J. Musgrove (1990), Topographic effects on flow path and surface water chemistry of the Llyn Brianne catchments in Wales, *J. Hydrol.*, *115*(1–4), 243–259, doi:10.1016/0022-1694(90)90207-E.

Zeng, F.-W., and C. A. Masiello (2010), Sources of CO_2 evasion from two subtropical rivers in North America, *Biogeochemistry*, *100*(1–3), 211–225, doi:10.1007/s10533-010-9417-6.